NASA Technical Memorandum 78804

NASA-TM-78804 19790006844

EFFECT OF HEAD-WIND PROFILES AND MEAN HEAD-WIND VELOCITY ON LANDING CAPACITY FLYING CONSTANT-AIRSPEED AND CONSTANT-GROUNDSPEED APPROACHES

Earl C. Hastings, Jr., and Wendell W. Kelley

January 1979

NASA
National Aeronautics and Space Administration

Langley Research Center
Hampton, Virginia 23665

SUMMARY

A study was conducted to determine the effect of head-wind profiles and mean head-wind velocities on runway landing capacity for airplanes flying constant-airspeed and constant-groundspeed approaches. It was determined that when the wind profiles were encountered with the currently used constant-airspeed approach method, the landing capacity was reduced. The severity of these reductions increased as the mean head-wind value of the profile increased. When constant-groundspeed approaches were made in the same wind profiles, there were no losses in landing capacity. In an analysis of mean head winds, it was determined that in a mean head wind of 35 knots, the landing capacity using constant-airspeed approaches was 13% less than for the no wind condition. There were no reductions in landing capacity with constant-groundspeed approaches for mean head winds less than 35 knots. This same result was observed when the separation intervals between airplanes was reduced.

INTRODUCTION

The need to increase airport landing capacity has led to the study of a number of advanced approach methods which offer the potential of airport capacity increases. A number of such techniques are discussed in reference 1, including dual vertical path approaches, dual vertical path-curved approaches, and reduced separation intervals.

Reference 2 has shown that the delivery precision available with 4D navigation systems (such as described in ref. 3) has the potential for

reducing arrival errors at the ILS gate. These navigation systems provide inputs to the autothrottle to change airspeed as required in order to maintain the required groundspeed. The constant-groundspeed method, as used in this study, utilizes a 4D navigation system and autothrottle capability to maintain a required groundspeed between the ILS gate and the landing flare manuever near the threshold. This technique differs from the current automatic landing system concept which utilizes the autothrottle to maintain constant airspeed during this segment of the approach.

A preliminary study which compared the landing capacity of the two approach methods in steady winds (ref. 4), indicated that in steady head winds the constant-groundspeed method offered significant benefits. More recent studies have considered the constant groundspeed approach method with variable head winds and these studies are discussed in this report.

SYMBOLS AND ABBREVIATIONS

Values are given in SI and U.S. Customary Units. Calculations were made in U.S. Customary Units.

FAA	Federal Aviation Administration
F_n	net thrust, N (lbf)
f_g	airspeed increment added for gusts, knots
h	height above ground level, or altitude, m (ft.)
ILS	instrument landing system
i	designates leading airplane in a pair

j	designates following airplane in a pair
P	proportions of airplanes of a certain type in a mix of airplanes
p_{ij}	probability of pair combination i-j
t	time, sec
$\bar{t}$	mean interarrival time, sec
t_{ij}	interarrival time between airplane i and airplane j, sec
V_A	airspeed, knots
V_g	groundspeed, knots
$\dot{V}_g$	rate of change of groundspeed with respect to time, m/sec^2
$\bar{V}_g$	mean groundspeed, knots
V_w	wind speed, knots
$\bar{V}_w$	mean wind speed, knots
ΔV_w	airspeed increment added for winds, knots
x	longitudinal distance between the threshold and a point on the extended runway centerline, km (n. mi.)
γ	length of approach path between the projected touchdown point and the ILS gate, km (n. mi.)
δ_F	flap position, deg
δ_{ij}	wake turbulence separtion interval between airplane i and j, km (n. mi.)
δ_{th_c}	incremental throttle position from trim, deg
δ_{th_o}	throttle position for trimmed flight at initiation of landing approach simulation, deg
Θ	body pitch attitude, deg
ρ	mass density of air, kg/m^3
σ	density ratio, $\frac{\rho}{\rho_{SL}}$

Subscripts:

c	control
gate	ILS gate
i	leading airplane in a pair
j	following airplane in a pair
max.	maximum
min.	minimum
ref.	reference
S.L.	sea level
td	touchdown

DESCRIPTION OF THE STUDY

Airplane and Automatic Landing Systems

Airplane. - Figure 1 shows a drawing of the Boeing 737-100 airplane which was modeled for the simulation study. The airplane is equipped with triple-slotted trailing-edge flaps, leading-edge slats, and Krueger leading-edge flaps. Longitudinal control is achieved by an elevator and trimmed by a movable stabilizer, and lateral control is obtained by combined ailerons and spoilers. A single-surface rudder provides directional control. The two turbofan engines are equipped with deflector doors for thrust reverse operation on the ground. Some charactertistics of the airplane are listed in Table I.

Automatic landing systems. - The simulated automatic approaches involved the use of three subsystems: an ILS glideslope tracking and flare

control system which uses the airplane elevator for pitch control, an airspeed-hold autothrottle which maintains a preselected airspeed throughout the landing approach, and a groundspeed-hold autothrottle which maintains a preselected groundspeed throughout the approach. The glideslope tracking and flare control system was used during both the airspeed-hold and groundspeed-hold autothrottle approaches.

The nominal approach profile common to all of the wind profile analysis is shown in figure 2. The x distance between the threshold and the ILS gate (the beginning of the final approach segment of an instrument approach) was -9.26 km. At the ILS gate, the glideslope height was 501.4 m.

The automatic landing (autoland) system was designed to intercept and track the glideslope, perform an automatic flare and touchdown, and lower the nose to the runway for the rollout phase. On a typical approach, the airplane approaches the glideslope in level flight from an altitude of approximately 500 - 1000 m. Just prior to glideslope interception, the autoland system lowers the nose and initiates a descent to intercept the glideslope beam.

Following beam interception, the glideslope tracking phase begins. During this phase, the beam error signals are augmented by inertial inputs to provide smooth and stable flight-path-angle control.

Glideslope tracking continues down to a specified altitude, at which time an automatic flare and touchdown are accomplished. Flare altitude is computed as a function of the airplane's vertical speed. Following touchdown, the nose is lowered to the runway for rollout.

A detailed discussion of the autoland control law is contained in the Appendix.

The airspeed-hold autothrottle system used in this study is described in detail in references 5 and 6. The control law is shown in figure 3. The system is designed to hold a control airspeed, V_{A_c}, which is selected by the pilot. (Selection of V_{A_c} is discussed in detail later.) During autothrottle operation, the difference between V_{A_c} and the actual airspeed, V_A, forms an error signal which is used as an acceleration command. This command is summed with longitudinal acceleration feedback from the inertial navigation system (modified by a shear detector circuit) and fed to an autothrottle integrator. The integrator output is actually an incremental throttle command since the throttles are driven from the position, δ_{th_o}, existing at the time of autothrottle engagement. The sum of δ_{th_o}, the integrator output and a scaled longitudinal acceleration signal forms the throttle command.

The shear detector circuit is essentially a complementary filter which utilizes true airspeed, $V_{A_{SL}}$, and inertial longitudinal acceleration to generate a signal which compensates for wind shears. The filter design causes steady-state winds to be washed out and turbulence to be filtered, so that only wind shears significantly affect the shear detector output. Therefore, the detector output gives a measure of the rate-of-change of airspeed due only to shear and inertial acceleration.

During flare, the shear detector outputs are not used and the throttle is reduced at a constant rate which results in approximately idle thrust at touchdown.

The groundspeed-hold autothrottle control law is shown in figure 4. In this design, the error signal is the difference between indicated groundspeed, V_g, and pilot-selected control groundspeed, V_{g_c}. This groundspeed error signal is then used as an acceleration command which is combined with $\dot{V}_g$ to form the throttle command.

During flare, the groundspeed-hold mode is interrupted as the throttles are reduced to idle for landing. The rate of throttle reduction is the same as for the airspeed-hold system. Therefore, the airspeed (and groundspeed) loss during flare are similar for the two autothrottle systems.

As a safety feature, a minimim airspeed, $V_{A_{min}}$, detector is included in the groundspeed-hold design. The purpose of this detector is to assure that V_A is not reduced to a value below that used for a normal (airspeed-hold) approach (V_{A_c}). If such a detector were not included in the design, it would be possible for the autothrottle to reduce V_A to a dangerously low value in an attempt to hold V_g constant. Such a siutation might exist in strong tail-wind or head-wind-shearing-to-tail-wind conditions.

Therefore, with the groundspeed-hold system used in this report, the pilot selects both V_{g_c} and $V_{A_{min}}$. In the event airspeed falls below $V_{A_{min}}$, autothrottle operation reverts automatically to the airspeed-hold mode (figure 3).

Wind Profiles

A number of wind profiles have been used by the FAA in piloted simulator tests of wind shear effects. Three of these were selected for this study, to assess the effects of winds in a realistic manner and are shown in figure 5. The mean value, $\bar{V}_W$, for each is also shown. Since this study was concerned with landing capacity in normal or nearly normal conditions profiles with mild wind shear characteristics were selected. Only the longitudinal wind components were analyzed since it is this component which primarily effects groundspeed and, consequently, the landing capacity. Since analysis showed that the presence of turbulence had a negligible effect on landing capacity, no turbulence was considered in the study.

It can be noted from figure 5 that all of the selected wind profiles were head winds. This was because routine landing operations normally take place in head winds rather than tail winds and also because, as noted, the automatic groundspeed-hold autothrottle system used in this study may revert to the automatic airspeed-hold autothrottle system in tail winds.

In the wind profile analyses, the simulated airplane flew automatic approaches between the ILS gate and touchdown. An approach was made in no wind conditions and in each of the wind profiles. In this study, approach flap deflections of 40° ($\delta_F = 40^{\circ}$) and 30° ($\delta_F = 30^{\circ}$) were considered. In all approaches the landing gear was extended, the speed brakes were retracted, and the weight was 37,195 kg (82000 lbm).

The control speeds for the approaches in the various wind environments and flap deflections are given for the constant airspeed method in Table II and for the constant groundspeed method in Table III. For the constant airspeed approaches the control airspeed, V_{A_c}, was determined using the procedure of reference 7 expressed by the equation

$$V_{A_c} = V_{A_{ref}} + \Delta V_w + f_g \qquad (1)$$

where $V_{A_{ref}}$ is a reference approach airspeed for a given weight and flap deflection, ΔV_w is an airspeed increment added for winds, and f_g is an airspeed increment added for gusts. Using the procedure of reference 7, ΔV_w was taken as half of the value of V_w at the surface (see fig. 5) and f_g was taken as zero since gusts were not used with the mild wind shears considered in this study.

The values of $V_{A_{ref}}$ in Table II were from reference 7 for the study aircraft at a weight of 37,195 kg. These approach airspeeds are a factor of 1.3 above the stall speeds in order to provide adequate manuevering capability during the approach. It will be noted that $V_{A_{ref}}$ at $\delta_F = 30^o$ is 5 knots greater than at $\delta_F = 40^o$ due to the change in stalling speed with flap setting.

The values of the control groundspeeds, V_{g_c}, for the constant-groundspeed approaches (Table III) were the same as the reference airspeeds, $V_{A_{ref}}$, in Table II. This selection was intended to minimize groundspeed losses in head winds without increasing the stopping distance requirements over the no-wind condition.

Analysis Methods

Simulation model. - The airplane simulation model was a representation of the study airplane previously described and shown in figure 1. The simulation program used nonlinear equations of motion and nonlinear aerodynamic characteristics including ground effect. Only the longitudinal degrees-of- freedom were simulated. Verification of the basic airframe simulation was accomplished by comparing model response to airplane response for longitudinal control inputs.

Simulation of the airplane control systems included a nonlinear representation of the engine thrust characteristics. Figure 6 (ref. 8) shows the total thrust characteristics representative of both airplane engines at landing approach speeds.

The simulation model also took into acount the variation of the density ratio, σ, with height above ground level (h). As the result, there was a density effect on V_A. For the no-wind condition, the density effect resulted in a value of V_g which was slightly greater than V_A for all altitudes above ground level. As will be noted, this effect was small in this study and did not significantly influence the analysis of the wind profiles.

Landing capacity analysis procedure. - As used in this report, the landing capacity, λ, is defined (as in reference 1) as the number of landing operations that a single runway can accommodate during an hour when there is a continuous demand to land and each available landing opportunity is filled. The capacity analysis procedure described in reference 1 was based on constant airspeeds since wind effects were not considered in that

analysis. In this study, the landing capacity analysis procedure was the same as reference 1 except that the mean groundspeed, $\bar{V}_g$, between the ILS gate and touchdown was used rather than a constant V_A.

The approach geometry for the landing capacity analysis is shown in figure 7. The interarrival times for each aircraft pair were determined from the equations:

$$t_{ij} = \frac{\delta_{ij}}{\bar{V}_{g_j}} \qquad V_{g_i} \leq V_{g_j} \quad (2)$$

$$t_{ij} = \frac{\delta_{ij}}{\bar{V}_{g_j}} + \gamma\left(\frac{1}{\bar{V}_{g_j}} - \frac{1}{V_{g_i}}\right) \qquad \bar{V}_{g_i} > \bar{V}_{g_j} \quad (3)$$

where γ is the length of the approach path. Note in figure 7 that when $\bar{V}_{g_i} \leq \bar{V}_{g_j}$, the distance δ_{ij} occurred at the runway (solid airplane symbols) and when $V_i > V_j$, the distance δ_{ij} occurred at the ILS gate (open aircraft symbols).

If it assumed that the landing sequence was random, the probabilities of each pair sequence i - j were given by

$$p_{ij} = P_i P_j \quad (4)$$

where P_i and P_j were proportions of the types of i and j airplanes in the mix.

After t_{ij}, and p_{ij} were determined for all possible pairs, the mean interarrival time $\bar{t}$ at the threshold was computed as;

$$\bar{t} = \Sigma\,(t_{ij}p_{ij}) \quad (5)$$

(where the sum is over all possible pairs), and the landing capacity in operations/hr, λ, was determined by the equation

$$\lambda = \frac{1}{\bar{t}} \quad 3600 \qquad (6)$$

RESULTS AND DISCUSSION

Effects of Wind Profiles on Airspeed and Groundspeed

Constant-airspeed approaches. - Figure 8 shows values of V_A and V_g during approaches in the no wind condition and in the wind profiles of figure 5. The data for the no wind condition in figure 8(a) shows the variable density effect noted earlier. This effect on V_g was small (+3 kts at the ILS gate diminishing to zero at touchdown) and was neglected in this analysis.

The data in figure 8 show several trends which are common to all of these approaches. In all of the wind profiles, V_g was less than for the no wind condition. During all approaches in the wind profiles V_g was also less than V_A. The magnitude of the difference between V_g and V_A at a given altitude, h, was proportional to V_w at that altitude (see fig. 5). At the lower altitudes ($h < 100$ m) where V_w decreased, the values of V_g approached those of V_A. At $h \approx 20$ m, the flare manuever occurred and both V_A and V_g decreased rapidly.

Since the value of V_{A_c} was greater with $\delta_F = 30^o$ than with $\delta_F = 40^o$ (Table II), values of V_g were correspondingly higher with $\delta_F = 30^o$. The variations in V_g caused by the wind profiles was the same with both flap deflections.

Of the three wind profiles shown in figure 8, the most adverse effects of winds, in terms of the difference between V_A and V_g are shown by profile 3 (fig. 8(d)). In this profile, V_g was approximately 40 kts less than V_A between the ILS gate and h = 100 m for both $\delta_F = 40^o$ and $\delta_F = 30^o$. At touchdown V_g was about 13 kts less than V_A for both flap deflections.

Table IV presents values of the mean groundspeed, $\bar{V}_g$ for these approaches. These values were determined from the expression

$$\bar{V}_g = \frac{X_{td} - X_{gate}}{t_{td} - t_{gate}} \tag{7}$$

Values of the mean windspeed, $\bar{V}_w$, and wind correction factors, ΔV_w, are also noted in Table IV.

These data show that, relative to the no wind condition, each of the profiles resulted in a reduction in $\bar{V}_g$ since ΔV_w was always less than $\bar{V}_w$. The reductions in $\bar{V}_g$ were proportional to $\bar{V}_w$. This trend is the same for both flap deflections. It should be noted, however, that the values of $\bar{V}_g$ are about 4 to 5 kts greater with $\delta_F = 30^o$ than with $\delta_F = 40^o$.

Constant-groundspeed approaches. - Values of V_A and V_g for these approaches are shown in figure 9. The data for the no wind condition in figure 9(a) show that the density effect on V_A was small (-3 kts at the ILS gate and diminishing the zero at touchdown) and this effect was neglected in this analysis.

Several trends which are common to all of these approaches can be noted in figure 9. During all approaches in the wind profiles, V_g was essentially the same as for the no wind condition and V_A was always

greater than for the no wind condition. In each profile, the increase in V_A relative to V_g at a given altitude, h, was proportional to the value of V_w at that altitude (fig. 5). As head wind increased, V_A increased and when V_w decreased at h < 100 m, V_A approached the value of V_g. The thrust reduction at h≈20 m resulted in a rapid decrease in V_A and V_g as was shown with the constant airspeed technique.

With $\delta_F = 30^o$, V_A in each profile was approximately 5 kts greater than $\delta_F = 40^o$ since V_{g_c} was greater by that amount. The variations in V_A due to the wind profiles were the same with both flap deflections.

The greatest increase in V_A due to winds was with profile 3 (fig. 9(d)). Between the ILS gate and h = 250 m, V_A was approximately 35 kts greater than V_g and at h = 150 m. V_A was about 40 kts greater than V_g. The low altitude wind shear of this profile caused a large decrease in V_A between h = 150 m and touchdown. Profiles 1 and 2 also show a significant decrease in V_A below h = 100 m.

It is important to note that these data show that with this approach method, airspeed reductions due to these low altitude wind shears do not reduce the manuever speed margin below the required value of 1.3. The presence of head winds along the approach path increases V_A, and consequently the manuever speed margin, above the required value. The reductions in V_A which result from decreasing head winds merely reduce the excess speed margin. As V_w decreased to zero, V_A decreased to $V_{A_{ref}}$ which is set by the required speed margin.

Table V presents a tabulation of the values of $\bar{V}_g$ with this approach method. The mean windspeeds, $\bar{V}_w$, are also shown. These data show that with both $\delta_F = 40^o$ and $\delta_F = 30^o$, there were no significant reductions in $\bar{V}_g$ relative to the no wind condition. It is also shown that at $\delta_F = 30^o$, $\bar{V}_g$ was about 5 kts greater than at $\delta_F = 40^o$ as it was the constant-airspeed approaches. It will be shown that, since these wind profiles did not reduce $\bar{V}_g$, significant landing capacity benefits were obtained with this approach method. The increase in $\bar{V}_g$ with partial flap deflection will also be shown to offer some landing capacity gains for both approach methods.

Operational Considerations for Constant-Groundspeed Method

Pitch attitude. - Data in figure 9 showed that, with the constant-groundspeed method, V_A may be considerably higher than normal due to the wind profile. This will result in pitch attitude changes which may be important to the flare and touchdown manuevers.

Figure 10 shows that all of the head-wind profiles resulted in a noticeably more negative (nose down) pitch attitude, Θ, than the no wind condition when $h > 100$ m. At $h < 100$ m the values of V_w decreased for these profiles and the values of Θ approached those observed for the no wind condition. As a result, the touchdown attitudes were acceptable ($\Theta > 0^o$) for all of these profiles.

It should be noted, however, that if the winds did not shear so that V_A decreased near the ground, a large nose down pitch attitude would result at flare ($h \approx 20$ m). An extrapolation of the Θ data in

figure 10 show that this value could be -4^{o} to -5^{o} at the flare initiation. In this situation, a touchdown attitude with $\Theta > 0^{o}$ might not be possible since the data show that the increment in Θ during the flare is about $+4^{o}$. This indicates that the pitch attitude change due to V_A may impose a limit on approach airspeed with this technique. It should be noted, however, that the severity of this effect is highly dependent on individual airplane configurations and systems, and the data in figure 10 should not be taken as typical.

The data in figure 10 also show that, in all of these wind profiles, the use of partial flap deflection resulted in a higher pitch attitude than full flap deflection. This should be generally true and indicates that the use of partial flap deflection is advantageous with this approach method, since it reduces the nose down pitch attitude at a given airspeed.

Maximum airspeed limitations of airplane systems. A second operational consideration introduced by the higher than normal airspeeds during constant-groundspeed approaches is the airspeed limitations of the airplane systems. Systems such as spoilers, flaps, and landing gear all have airspeed limits which may be close to the values of V_A which the airplane may experience in these approaches. For example, the airplane used in this study experienced V_A = 161 kts while making an approach with $\delta_F = 40^{o}$

in wind profile 3 (fig. 9(d)). Reference 7 specifies that the maximum airspeed for this flap at $\delta_F = 40^0$ is 170 kts.

These data illustrate that landing systems airspeed limits, as well as the previously noted body pitch attitude at flare, must be considered when making constant-groundspeed approaches.

Landing Capacity

Effect of wind profiles. - The mean groundspeeds in Tables IV and V were used to determine the effect of the wind profiles on the landing capacity, λ. The results are shown in figure 11. These data are for a 9.25 km track length and a wake turbulence separation interval of 5.56 km (the interval currently required for airplanes of the type used in this analysis).

The data in figure 11 show that there were no reductions in λ due to the wind profiles with the constant-groundspeed method since there were no reductions in $\bar{V}_g$ (Table V). With the constant-airspeed method, λ was less in all of the wind profiles than it was for the no wind condition since ΔV_w was always less than $\bar{V}_w$ (Table IV). It can be noted in figure 11 that the greater the value of $\bar{V}_w$, the greater the reducted in λ. These results show the same trend as the steady-state analysis of reference 4.

When $\delta_F = 30^0$, the values of λ for both approach methods were one to two operations/hr greater than for an approach in the same environment with $\delta_F = 40^0$ since $\bar{V}_g$ was about 5 kts greater with

$\delta_F = 30^o$. The effect of the wind profiles on λ (relative to the no wind condition), however, were the same regardless of the flap deflection used.

Effects of mean wind velocity. - The preceeding landing capacity analysis dealt with three specific wind profiles and a specific commercial jet airplane. That analysis showed that for these wind profiles and airplane characteristic, λ decreased with increasing $\bar{V}_w$ with the constant airspeed method but was unaffect by $\bar{V}_w$ with the constant groundspeed method. The landing capacity analysis of the effects of mean wind velocity which is discussed in this part of the report is similar to that in reference 4. It was not limited to specific profiles but covered a range of $\bar{V}_w$ values from 0 to 50 kts. In addition, this study used a more typical mix of landing airplanes and separation intervals. This analysis also considered the operational limitations of airspeed which were not involved in the preceeding analysis.

Table VI lists the conditions of this analysis. A mix of commercial jet airplanes making a 9.25 km approach was analyzed. The mix contained 60% airplanes classified as type L (Large) and 40% airplanes classified as type H (Heavy). The type L aircraft all had takeoff weights between 5670 kg (12,500 lbm) and 136,078 kg (300,000 lbm). The type H airplanes all had takeoff weights exceeding 136,078 kg. The current wake avoidance separation intervals used in the analysis are also listed in Table VI for the possible airplane pair combinations.

Because of the previously noted advantages of partial flaps, the values of $V_{A_{ref}}$ in Table VI were chosen for this configuration. All type L airplanes had $V_{A_{ref}}$ = 140 knots and all type H airplanes had $V_{A_{ref}}$ = 145 knots. For constant airspeed approaches the limit airspeed, $V_{A_{max}}$, was defined as $V_{A_{ref}}$ + 20 kts as in reference 7 for the study airplane. Pitch attitude data in reference 4 were used to define $V_{A_{max}}$ for the constant groundspeed approaches as $V_{A_{ref}}$ + 35 kts.

The mean groundspeeds required for the capacity analysis (equations (2) and (3))were determined from the equation

$$\bar{V}_g = V_{A_{ref}} - \bar{V}_w + \Delta V_w \tag{8}$$

For the constant-airspeed approaches, ΔV_w was taken as half of the value of $\bar{V}_w$ but was limited to 20 kts. For the constant-groundspeed approaches ΔV_w was determined from

$$\Delta V_w = \bar{V}_w \quad \text{when } \bar{V}_w \leq (V_{A_{max}} - V_{A_{ref}}) \tag{9}$$

$$\Delta V_w = V_{A_{max}} - V_{A_{ref}} \quad \text{when } \bar{V}_w > (V_{A_{max}} - V_{A_{ref}}) \tag{10}$$

In order to establish the accuracy of the mean groundspeed, $\bar{V}_g$ as computed from equation (8) in this analysis, the results of the previous wind profile analysis were used. Values of $V_{A_{ref}}$, ΔV_w and $\bar{V}_w$ in Tables II through V were used to compute $\bar{V}_g$ from equation (8) and the results were compared with $\bar{V}_g$ values determined from the wind profiles by equation (7). The difference between the values was always less than 1 knot and showed that no significant error in λ was introduced by $\bar{V}_g$ in this analysis method.

The results of the analysis are shown in figure 12. As in the preceeding analysis of wind profiles, the constant-airspeed method resulted in capacity losses which increased as $\bar{V}_w$ increased. At $\bar{V}_w$ = 35 kts. λ was 13% less than at $\bar{V}_w$ = 0. With the constant-groundspeed method there were no losses in λ at values of $\bar{V}_w$ < 35 kts. The data in this figure also shows the importance of a large value of $V_{A_{max}}$, particularly with the constant-ground speed method. Increasing $V_{A_{max}}$ with this method increases the value of $\bar{V}_w$ which may be accommodated without a reduction in λ.

The significance of $V_{A_{max}}$ on λ with the constant-groundspeed method can also be noted by a comparison of the data in figures 11 and 12. In the analysis of the wind profiles, the data in figure 11 show that there was no loss in λ at $\bar{V}_w$ = 37.2 kts while the results of the mean wind analysis in figure 12 show that λ began to decrease at $\bar{V}_w$ = 35 kts. This is because the value of $V_{A_{max}}$ for the study airplane used in the analysis of the profiles was greater than the assumed values in Table VI for the mean wind analysis. As noted earlier, $V_{A_{max}}$ for the study airplane was 170 kts as imposed by the flap retraction airspeed limit. Thus $V_{A_{max}}$ was 50 kts greater than $V_{A_{ref}}$ for $\delta_F = 40^o$ and 45 kts greater than $V_{A_{ref}}$ for $\delta_F = 30^o$. As a result λ would begin to decrease at either $\bar{V}_w$ = 50 kts or $\bar{V}_w$ = 45 kts, depending on δ_F. In the analysis of the mean winds, however, $V_{A_{max}}$ was 35 kts greater than $V_{A_{ref}}$ (Table VI) and the reduction in λ, as seen in figure 12, began at $\bar{V}_w$ = 35 kts.

Effect of separation interval and path length. - The preceeding analysis utilized the current separation intervals from Table VI. Since reduced intervals have been shown to increase capacity and may be used

in the future (refs 1 and 2) an additional analysis was performed to evaluate the effect of reducing the current intervals. Data in figure 13 show λ for the two approach methods using δ_{ij} = 3.70 km (2 n. mi.) as a common separation interval between all airplane pairs.

The data in figure 13 show that, as with the current separation intervals, λ decreased with increasing $\bar{V}_w$ for the constant-airspeed methods. With the constant-groundspeed method there was no reduction in λ at $\bar{V}_w < 35$ kts. At $\bar{V}_w$ = 35 kts, the value of λ with the constant-airspeed method was 13% less than with the constant-groundspeed method. This result was the same as with current separation intervals and shows that the constant-groundspeed method has application in future terminal area operations which may utilize reduced intervals as well as those using the current intervals.

An analysis was also performed to define the effects of the length of the approach path, γ. In all of the preceeding analyses γ has a value of 9.25 km (5 n. mi.). It was found that, with current δ_{ij} values, reducing γ to 5.56 km (3 n. mi.) increased λ less than 1% and increasing γ to 12.97 km (7 n. mi.) reduced λ less than 1%. This result is consistent with that noted in references 1 and 4 for earlier capacity studies.

The relative insensitivity of λ to changes in γ in these analyses is because the values of $\bar{V}_g$ for the i and j airplanes are not widely different and the increase in t_{ij} between the fast-slow pairs (equation 3) due to changes in γ are not significant. Another contributing factor is that for the landing mix used in this study, fast-slow airplane pairs occurred only 24% of the time.

CONCLUDING REMARKS

Results have been presented of analyses of the effects of approach method on landing capacity for approaches conducted in head winds. Three wind profiles and various mean head-wind values were considered and the results have been compared with the no wind condition. Several operational considerations resulting from differences in the two approach techniques have also been shown.

The results showed that, with the currently used constant-airspeed approach method, the wind profiles resulted in losses in runway landing capacity which were proportional to the mean head-wind value of the profiles. The method which used constant-groundspeed during approaches, in the same wind profiles, resulted in no losses in landing capacity in these wind profiles.

In the analysis of the effect of mean head winds, the constant-groundspeed method resulted in no losses in landing capacity for mean head winds below 35 kts. At this mean head wind, the landing capacity using constant-airspeed approaches was 13% less than for the no wind condition. This same result was noted when the wake avoidance separation intervals were reduced between approaching airplanes. This indicates that this method is applicable to future as well as current terminal area operations.

Constant-groundspeed approaches in the study wind profiles resulted in considerably higher than normal approach airspeeds. It was shown that

it may be necessary to limit these airspeeds or flap deflections in order to avoid exceeding airspeed limitiation on flaps, spoilers, etc., and to avoid unacceptable pitch attitudes at flare initiation and touchdown.

APPENDIX

PITCH AUTOLAND CONTROL LAW DESCRIPTION

Symbols and Abbreviations

ALCT	elevator command used to intercept and track the ILS glideslope beam (trailing-edge down, positive), deg
FLARE	logic switch used to initiate elevator commands for flare
GSE	deviation from glideslope beam (above beam, positive), deg
GSEGP	deviation from glideslope beam, adjusted to provide signal de-sensitizing as altitude is reduced (above beam, positive), deg
GSTRK	logic switch used to initiate glideslope tracking mode
h_{RAD}	height above ground, measured by radar altimeter (always positive), m
$\dot{h}$	airplane vertical speed (climbing, positive), m/sec
$\ddot{h}$	airplane vertical acceleration (upward, positive), m/sec^2
HDER	flare height detection signal
ILS	instrument landing system
INS	inertial navigation system
V_g	airplane groundspeed, knots
δ_{e_c}	elevator command (trailing-edge down, positive), deg
$\dot{\Theta}$	pitch rate (nose up, positive), deg/s

Discussion

The ILS autoland system longitudinal control laws are shown in figure 14. On a typical approach, the airplane approaches the glideslope in level flight

from an altitude of approximately 500 - 1000 m. The control laws are engaged when the ILS glideslope receiver indicates a signal deviation (GSE) of ±0.108 deg or smaller. At that time, the autoland system commands a nose-down pitch change to intercept the glideslope beam.

Ten seconds after the control laws are engaged, the glideslope track (GSTRK) mode is activated which provides inertial flight-path augmentation to the ILS beam-error signal. Augmentation is provided by $\dot{h}$ and INS-derived V_g signals, which produce elevator commands to correct any deviations from a ground-referenced -3^o flight-path angle. The use of ILS beam-error and INS augmentation signals together results in accurate glideslope tracking in adverse wind conditions and in the presence of ILS beam disturbances. Vertical acceleration ($\ddot{h}$) and pitch-rate ($\dot{\Theta}$) feedback provide additional stability augmentation throughout the approach.

As the aircraft descends below an altitude of 50 m, flare detection computations are initiated. The flare detector uses a combination of radar altitude (h_{RAD}) and $\dot{h}$ signals to detect the proper flare height. Flare is initiated at the moment the HDER signal becomes negative. As an example, assume the aircraft is tracking the glideslope with a -3.5 m/sec rate of descent. In this case the HDER signal will be positive for all altitudes above 17.3 m, and as the airplane descends through 17.3 m, the HDER signal becomes negative and flare is initiated. If the rate of descent were higher, flare would start at a higher altitude. Correspondingly, flare would occur at a lower altitude for slower descent rates. A ramp elevator signal is used to start the nose up for the flare maneuver.

It should be noted that the HDER signal, in addition to initiating flare, also commands a sink rate which is programmed as a function of altitude. The purpose of the 4.57 m bias altitude signal is to achieve a predetermined sink rate at touchdown. For example, at zero altitude, a vertical speed of -0.73 m/sec is required to null the HDER signal. Thus, -0.73 m/sec is the desired vertical speed at touchdown.

REFERENCES

1. Hastings, Earl C. Jr., and Taylor, Robert T., Effects of Landing Approach Methods and Separation Intervals on Single Runway Landing Capacity, NASA Technical Paper 1112, 1977.

2. Harris, Richard M., Future ATC Technology Improvements and the Impact on Airport Capacity. Plans and Developments for Air Traffic Systems, AGARD-CP-188, May 1975.

3. Knox, Charles E., Experimental Determination of the Navigation Error of the 4-D Navigation, Guidance, and Control Systems on the NASA B-737 Airplane, AGARD-CP-240, October 1977.

4. Hastings, Earl C. Jr., A Preliminary Study of the Benefits of Flying by Groundspeed During Final Approaches: NASA TM 78777, August 1978.

5. Lambregts, A. A.: Turbulence Compensated Throttle Control System. U.S. Patent No. 3892374, 1975.

6. Lambregts, A. A.: Wind Shear Detection System. U.S. Patent No. 3955071, 1976.

7. Operations Manual Volume 1 Boeing Model 737-100, D6-27370-100 November, 1973

8. Hansen, R., and Tobie, H. N.: NASA TCV B-737 AGCS Nonpiloted Analog Computer Simulation. Doc. D6-44359TN, Boeing Company, 1977.

TABLE I. - CHARACTERISTICS OF AIRCRAFT USED IN THE STUDY

General:		
Length, m (ft)	28.65	(94.0)
Height to top of vertical fin, m (ft)	11.28	(37.0)
Wing:		
Area, m^2 (ft^2)	91.04	(980)
Span, m (ft)	28.35	(93.0)
Mean aerodynamic chord, m (ft)	3.41	(11.2)
Incidence angle, deg	1.0	
Aspect ratio	9.07	
Dihedral, deg	6	
Sweep, deg	25	
Flap area, m^2 (ft^2)	14.94	(160.8)
Weight, kg (lbm)	37,195	(82,000)
Inertia, kg-m^2 (slug-ft^2)		
roll	508,432	(375,000)
pitch	1,079,147	(795,938)
yaw	1,659,521	(1,224,000)
roll-yaw product of inertia	70,502	(52,000)
Center of gravity, percent of mean aerodynamic chord	20	

TABLE II: CONTROL AIRSPEEDS FOR CONSTANT-AIRSPEED APPROACHES

Wind Profile	δ_F deg,	$V_{A_{ref}}$ kts	ΔV_w kts	V_{A_c} kts
No Wind	40	120	0	120
1	40	120	0	120
2	40	120	0	120
3	40	120	5	125
No Wind	30	125	0	125
1	30	125	0	125
2	30	125	0	125
3	30	125	5	130

TABLE III: CONTROL GROUNDSPEEDS FOR CONSTANT-GROUNDSPEED APPROACHES

Wind Profile	δ_F def	V_{g_c} kts
No Wind	40	120
1	40	120
2	40	120
3	40	120
No Wind	40	125
1	40	125
2	40	125
3	40	125

TABLE IV: MEAN GROUNDSPEED FOR CONSTANT-AIRSPEED APPROACHES

δ_F deg	Wind Profile	ΔV_w kts	$\bar{V}_w$ kts	$\bar{V}_g$ kts
40	No Wind	0	0	121.2
40	1	0	16.7	104.3
40	2	0	21.4	99.5
40	3	5	37.2	88.6
30	No Wind	0	0	126.3
30	1	0	16.7	109.4
30	2	0	21.4	104.7
30	3	5	37.2	93.6

TABLE V: MEAN GROUNDSPEED FOR CONSTANT-GROUNDSPEED APPROACHES

δ_F deg	Wind Profile	$\bar{V}_w$ kts	$\bar{V}_g$ kts
40	No Wind	0	119.8
40	1	16.7	119.8
40	2	21.4	120.0
40	3	37.2	120.1
30	No Wind	0	124.7
30	1	16.7	124.8
30	2	21.4	124.9
30	3	37.2	124.9

TABLE VI: CONDITIONS FOR ANALYSIS OF EFFECT OF MEAN WIND VELOCITY

Airplane Type	Takeoff Weight kg	Percent type in landing mix	$V_{A_{ref}}$ kts	$V_{A_{max}}$ kts		Current separation intervals		
				Constant-airspeed method	Constant-groundspeed method	Airplane i	Airplane j	δ_{ij} km (n. mi.)
L (Large)	5,670 to 136,078	60	140	160	175	L	L	5.56(3)
						L	H	5.56(3)
H (Heavy)	greater than 136,078	40	145	165	180	H	L	9.25(5)
						H	H	7.40(4)

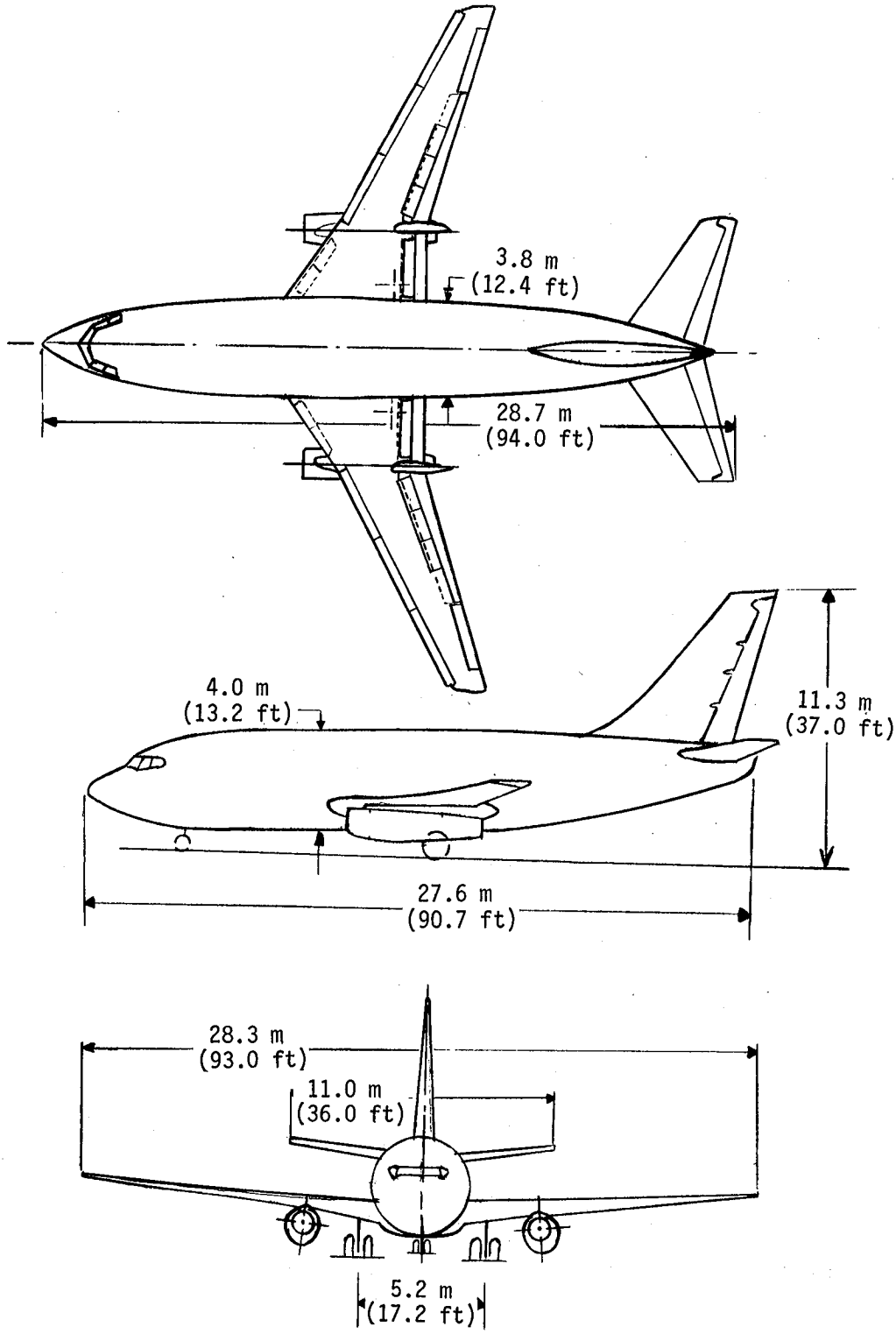

Figure 1. - Drawing of the B-737 airplane modeled in the simulation study.

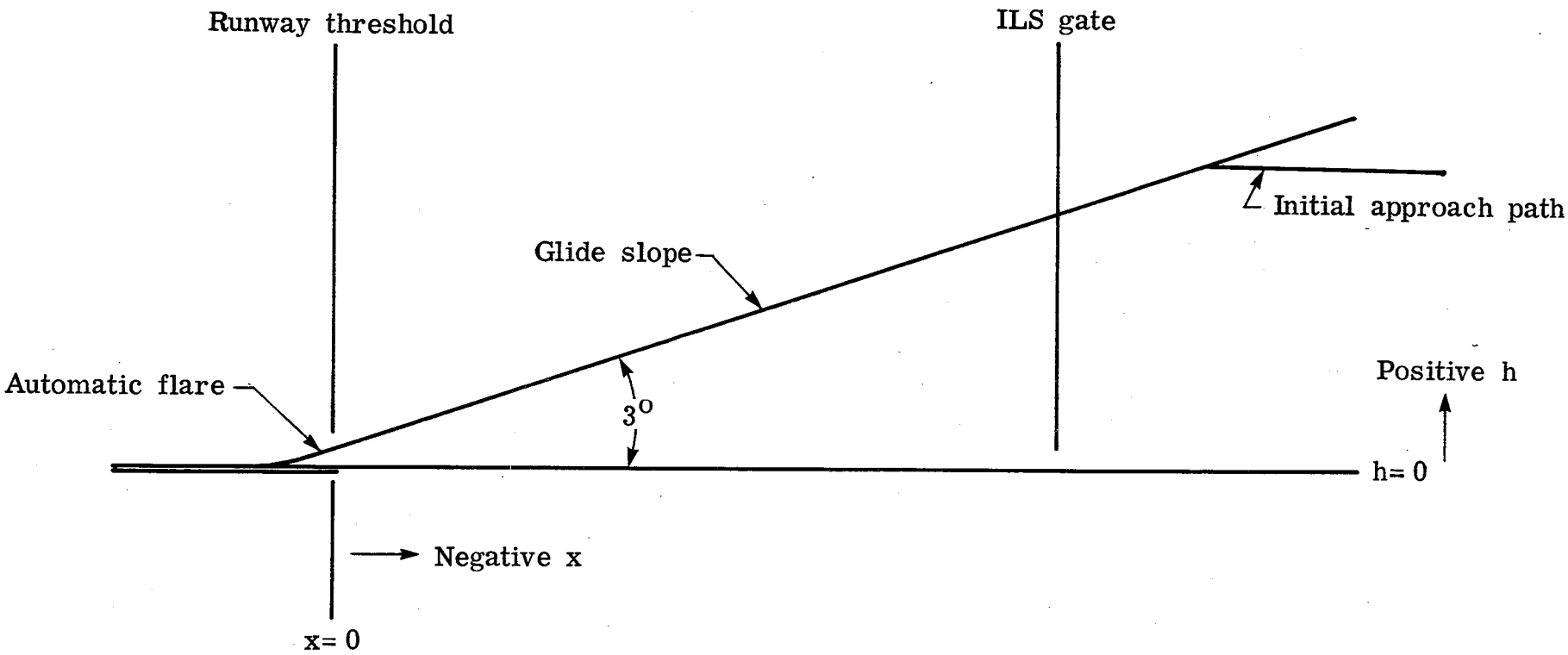

Figure 2.- Nominal approach profile.

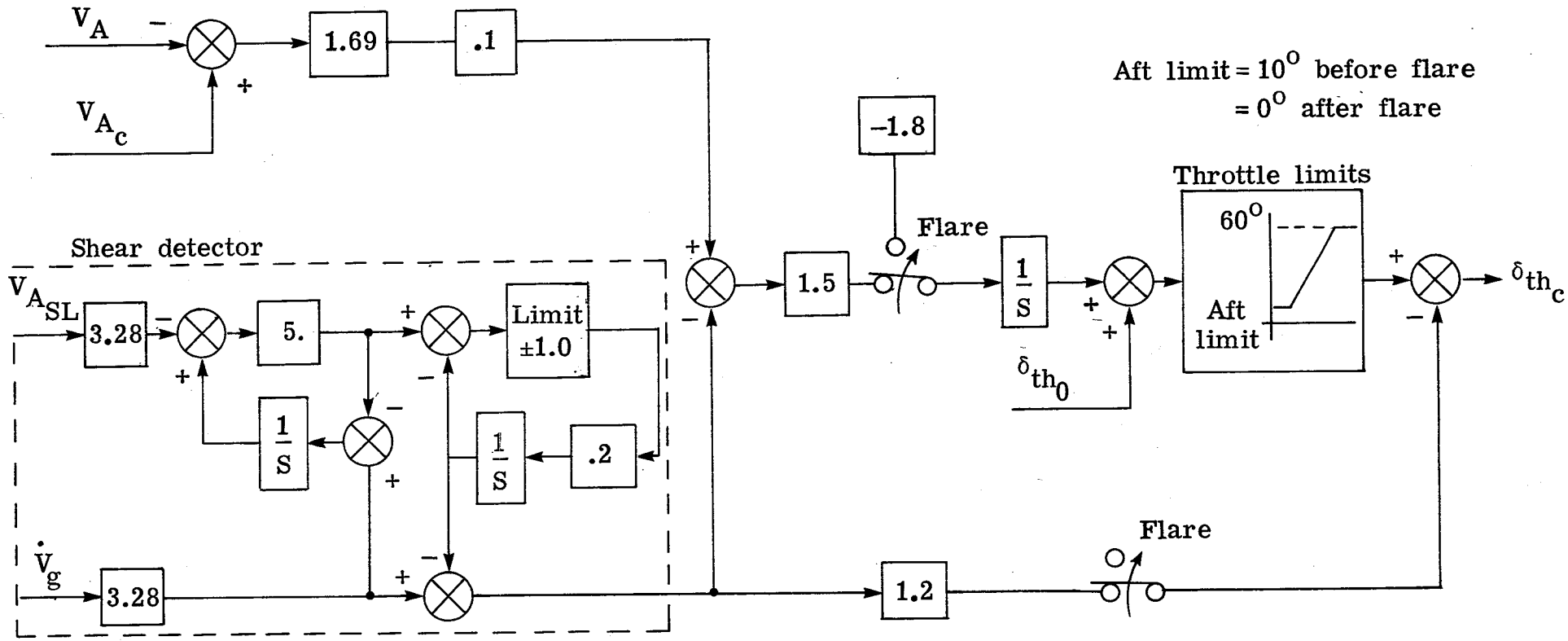

Figure 3.- Airspeed-hold autothrottle control law.

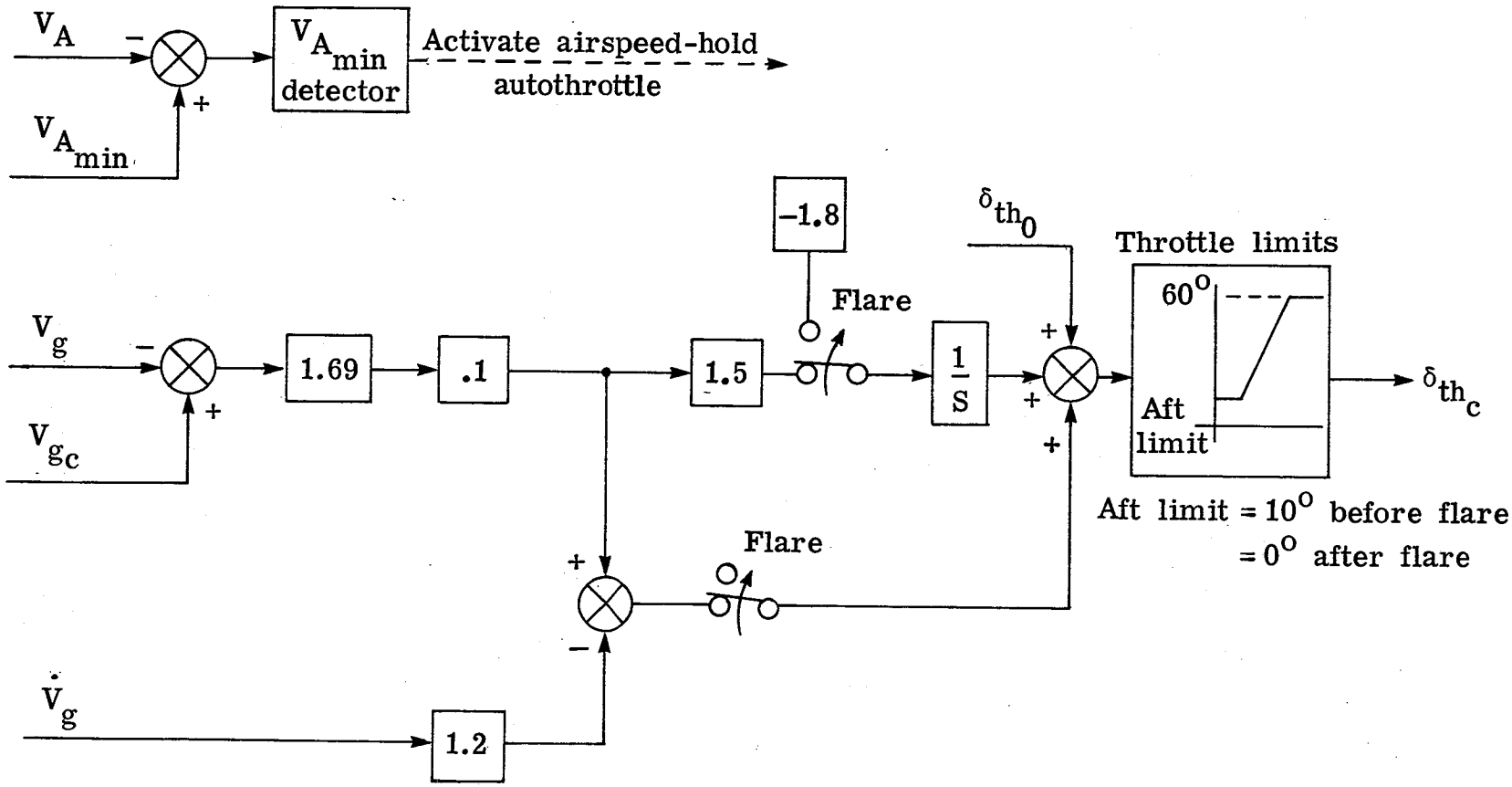

Figure 4.- Groundspeed-hold autothrottle control law.

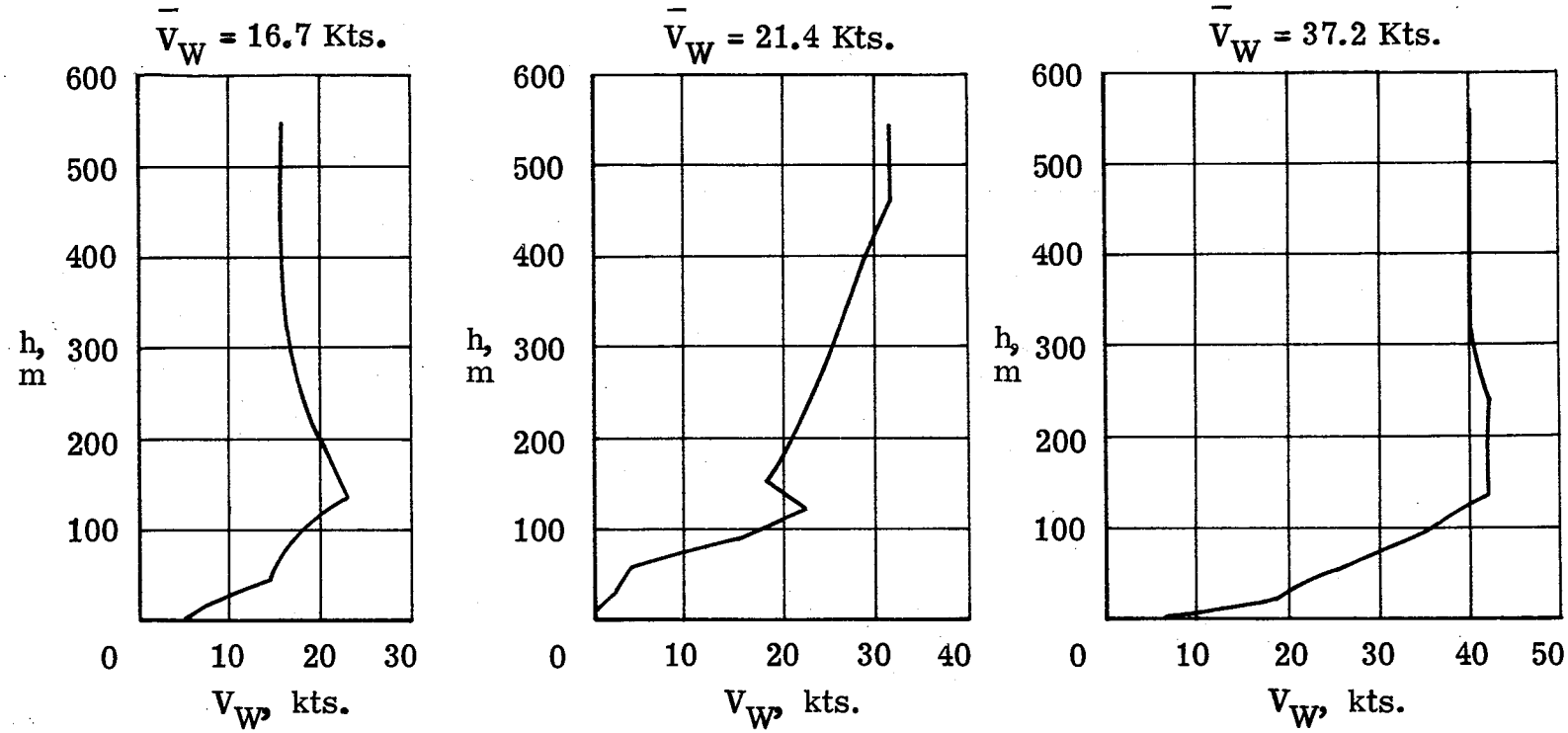

(a) Profile 1 (b) Profile 2 (c) Profile 3

Figure 5.- Wind profiles.

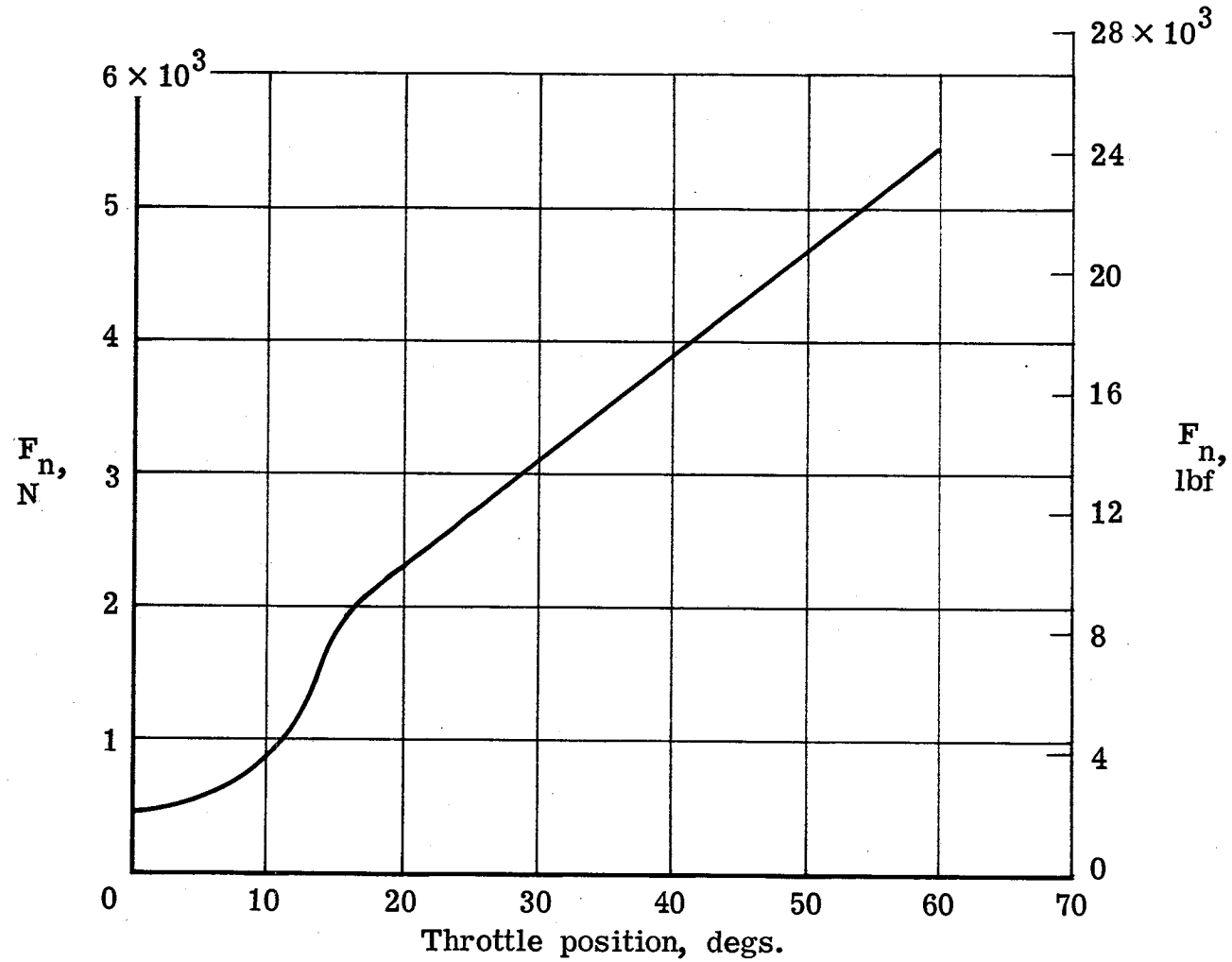

Figure 6.- Total thrust characteristics of the study airplane (both engines).

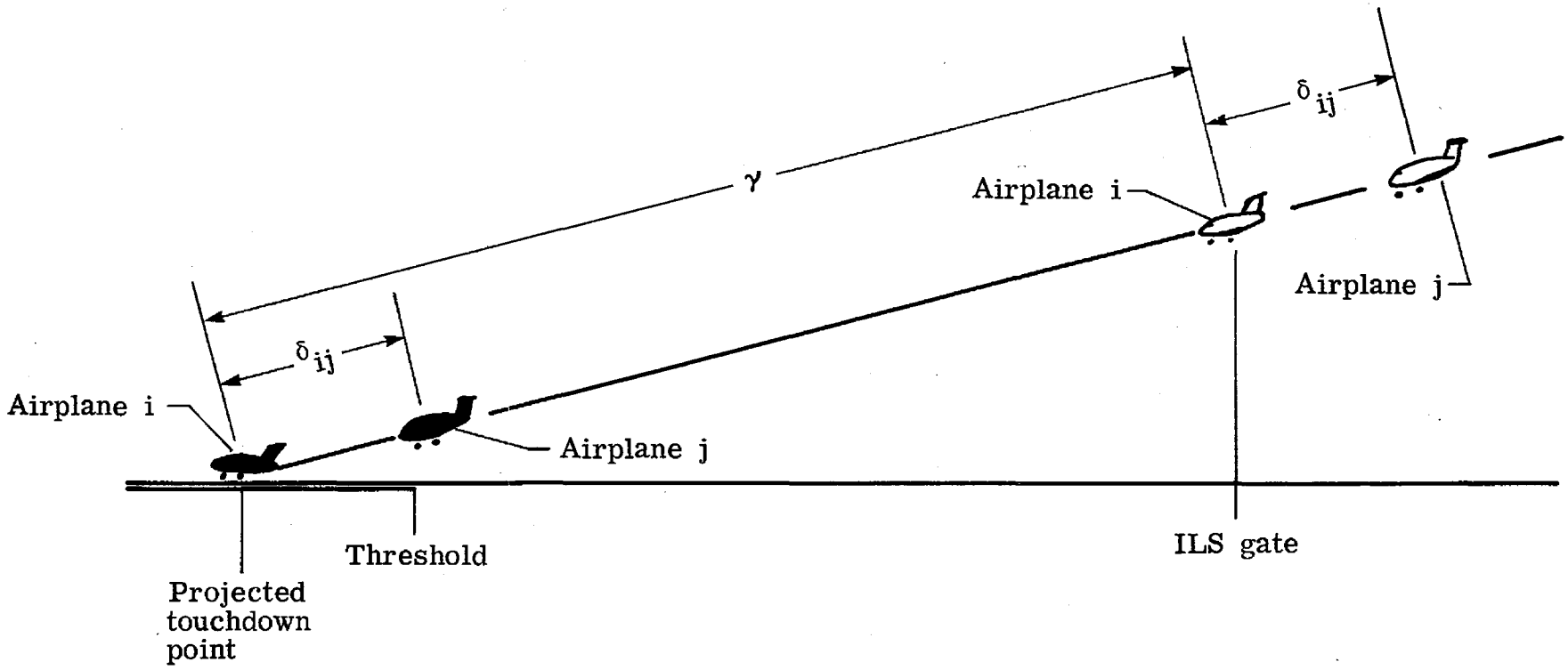

Figure 7.- Geometry used in the capacity analysis.

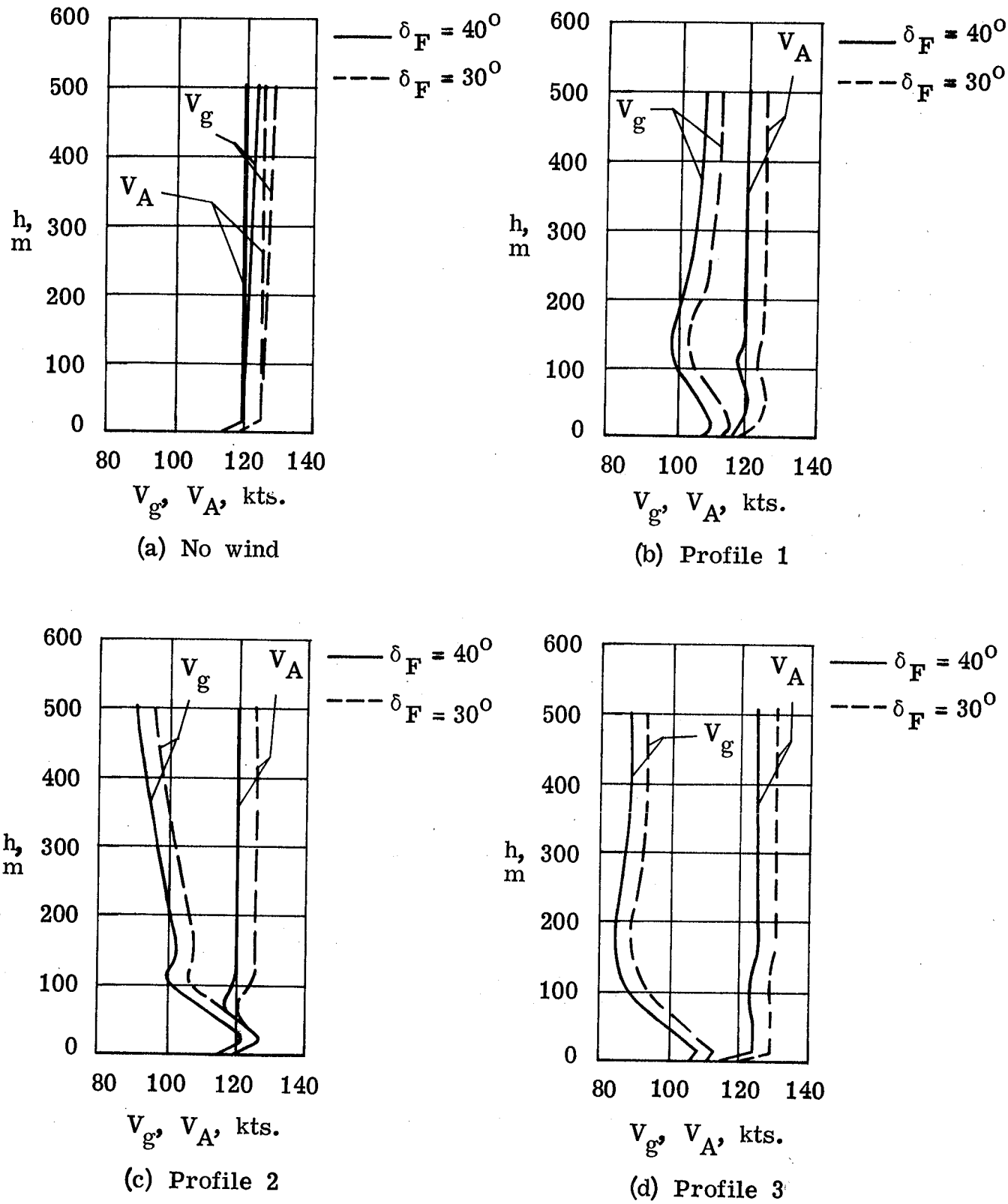

Figure 8.- Variations of groundspeed and airspeed for the constant-airspeed autothrottle law.

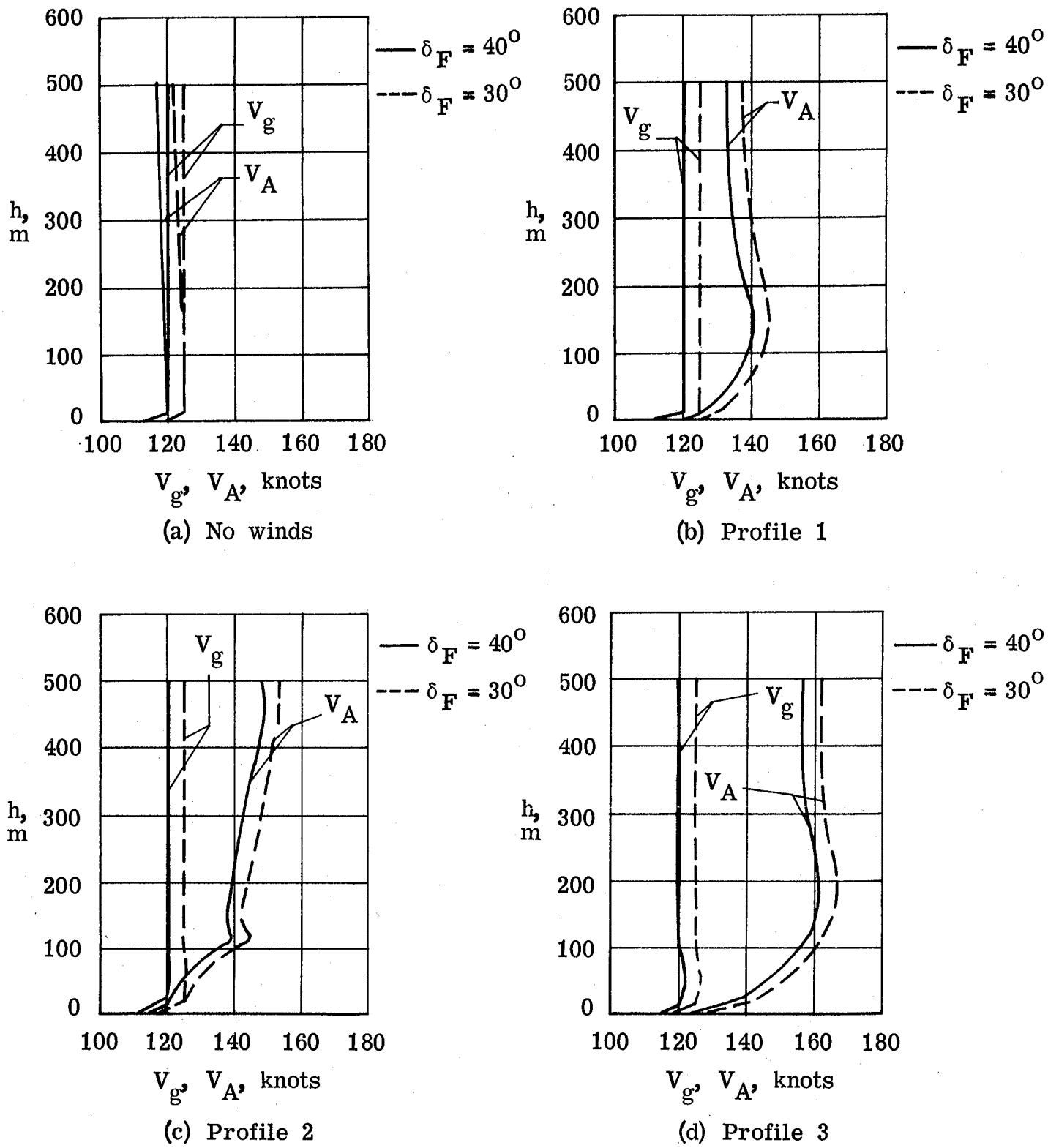

Figure 9.- Variations of airspeed and groundspeed for the constant-groundspeed autothrottle law.

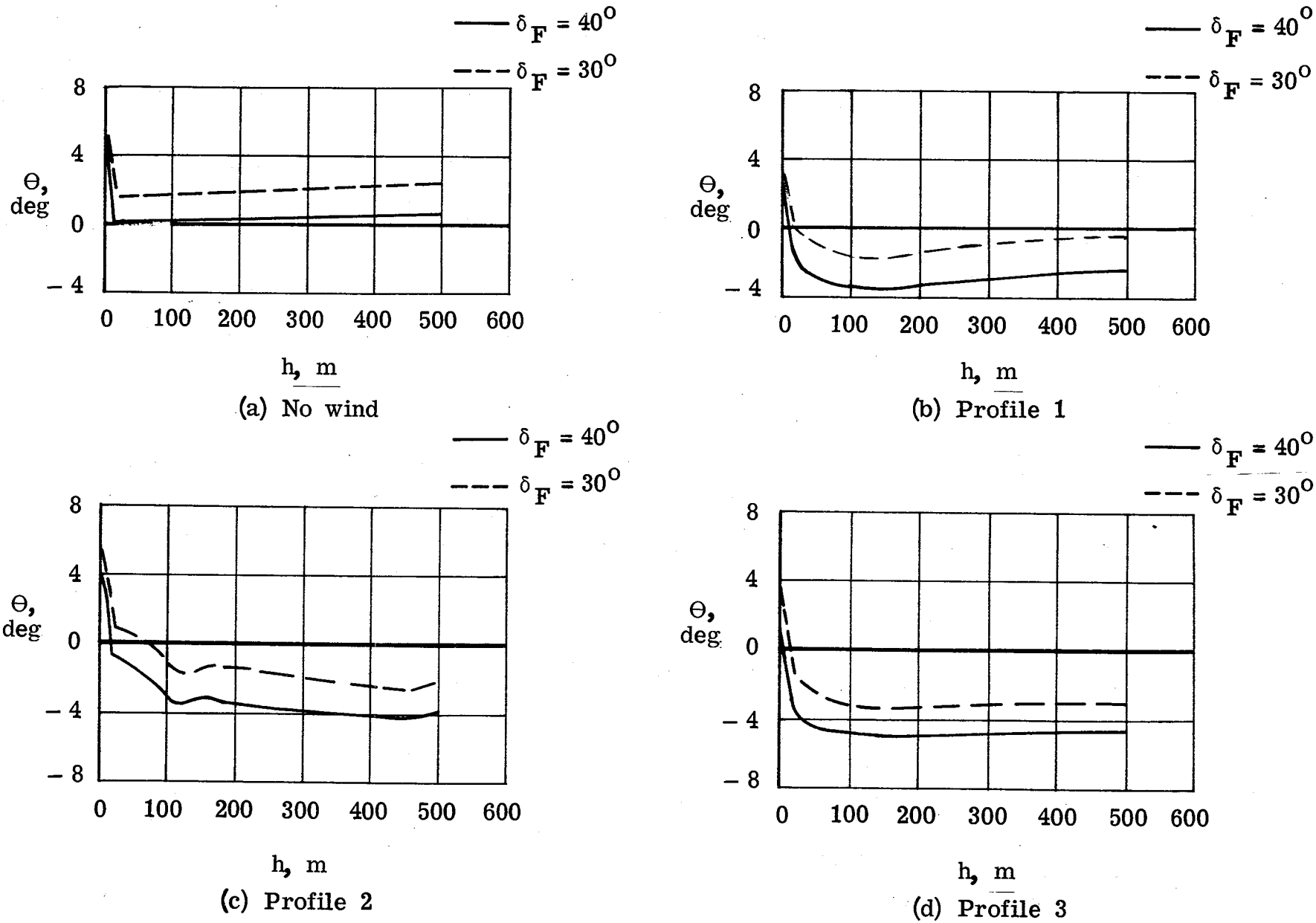

Figure 10.- Body pitch attitude for constant-groundspeed approaches.

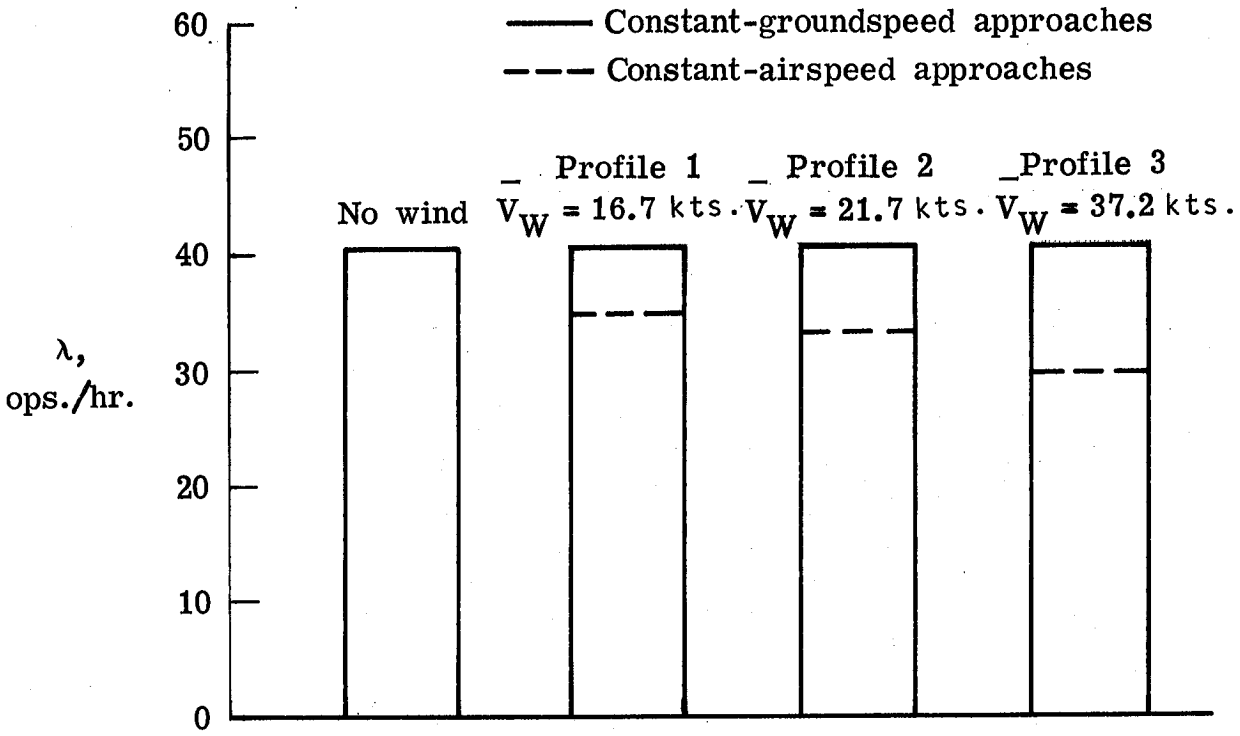

(a) $\delta_F = 40^o$

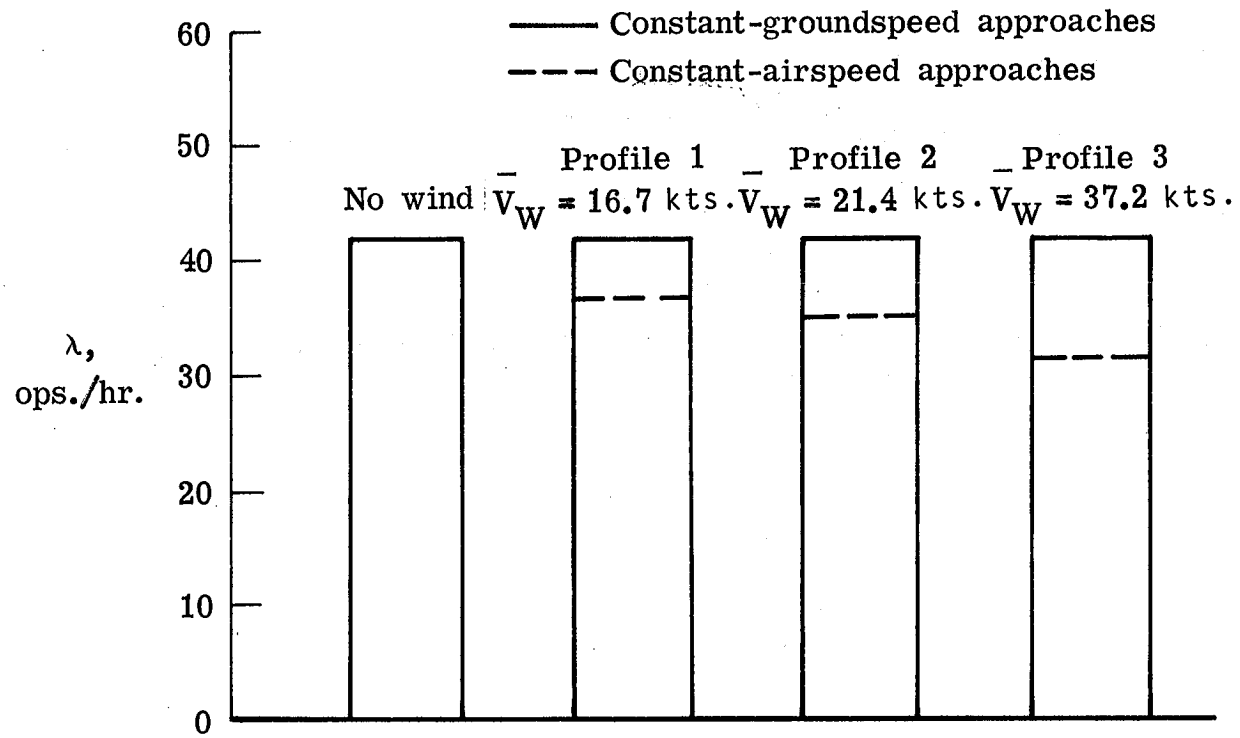

(b) $\delta_F = 30^o$

Figure 11.- Effect of wind profiles on landing capacity.

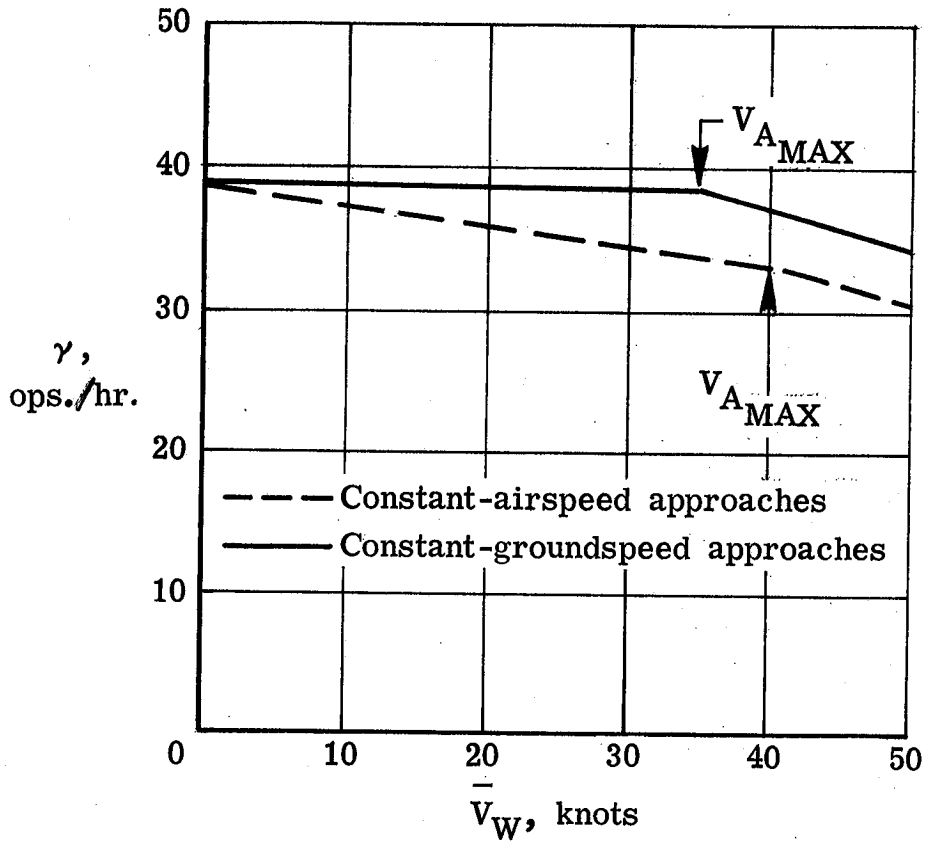

Figure 12.- Effect of mean head-wind velocity on landing capacity (current separation intervals).

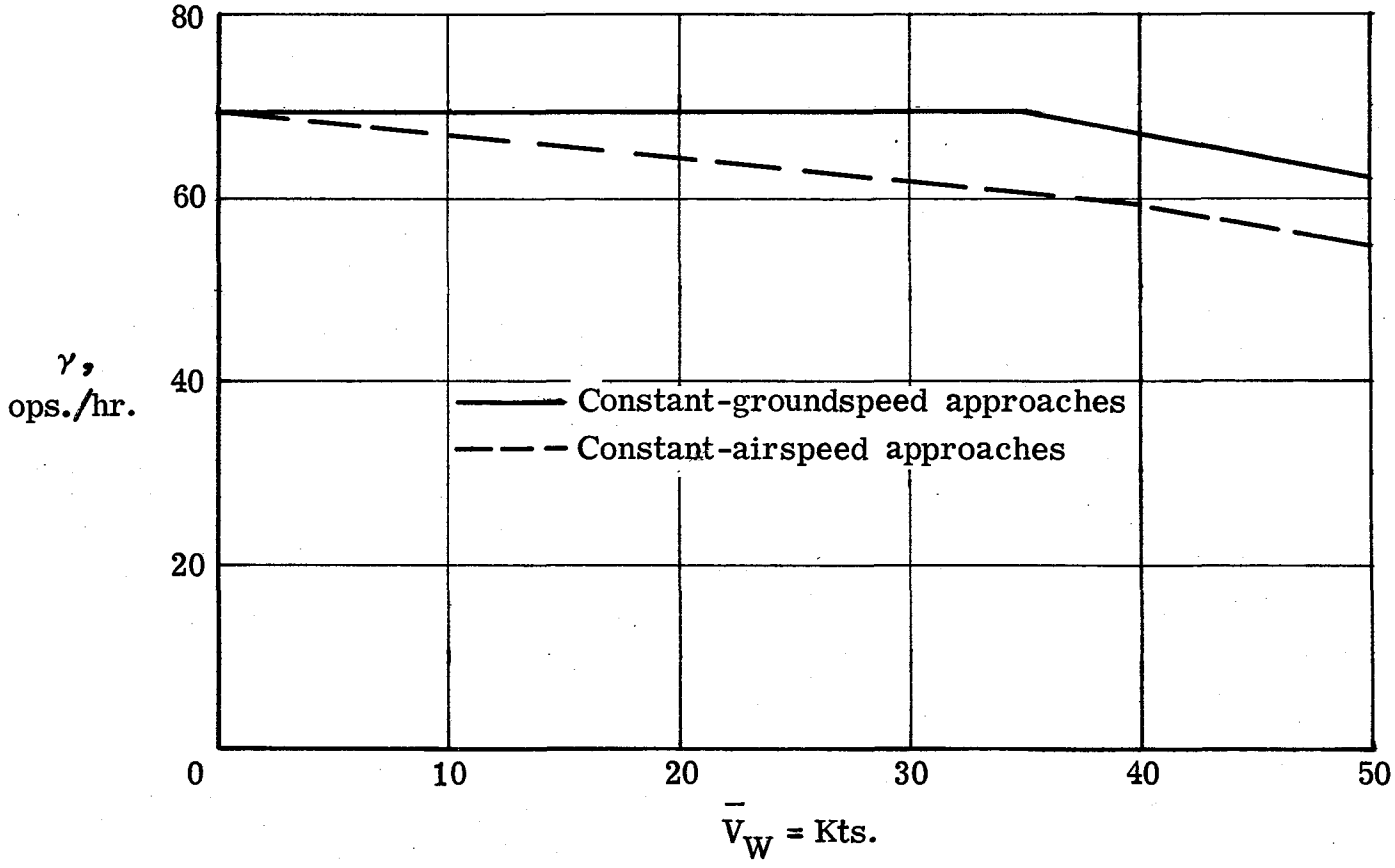

Figure 13.- Effect of mean head-wind velocity on landing capacity (reduced separation intervals).

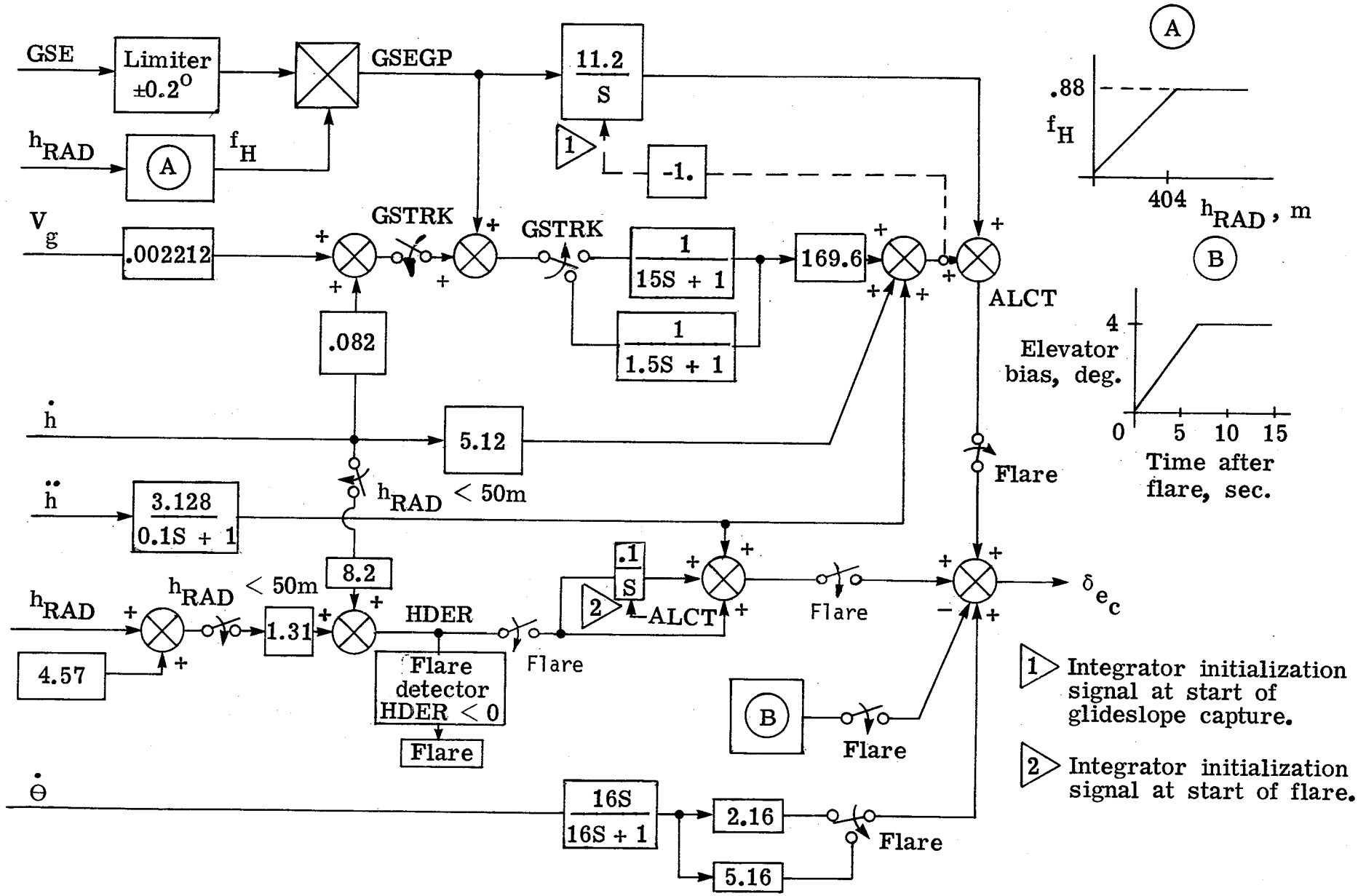

Figure 14.- Glideslope tracking and flare control laws.

1. Report No.	2. Government Accession No.	3. Recipient's Catalog No.
NASA TM 78804		

4. Title and Subtitle	5. Report Date
Effect on Head-Wind Profiles and Mean Head-Wind Velocity on Landing Capacity Flying Constant-Airspeed and Constant-Groundspeed Approaches	January 1979
	6. Performing Organization Code
7. Author(s)	8. Performing Organization Report No.
Earl C. Hastings, Jr., and Wendell W. Kelley	
	10. Work Unit No.
9. Performing Organization Name and Address	RTR 513-52-01-31
NASA Langley Research Center Hampton, VA 23665	11. Contract or Grant No.
	13. Type of Report and Period Covered
12. Sponsoring Agency Name and Address	Technical Memorandum
National Aeronautics and Space Administration Washington, DC 20546	14. Sponsoring Agency Code

15. Supplementary Notes

16. Abstract

A study of the effects of wind profiles and mean head-wind velocities on landing capacity was conducted. It was determined that when these conditions were encountered with the currently used constant-airspeed approach method, landing capacity losses resulted. The severity of these losses increased as the mean head-wind value increased.

When constant-groundspeed approaches were used in the same wind profiles there was no reduction in landing capacity. The study showed that in a mean head wind of 35 knots, the landing capacity using this method was 13% greater than with the constant-airspeed method. The same result was noted when separation intervals were reduced.

The constant-groundspeed approach method was found to result in significantly greater than normal approach airspeeds. This effect requires consideration of the airplane's flare capability at reduced pitch attitude, as well as consideration of the airspeed limits of the airplane systems.

17. Key Words (Suggested by Author(s))
landing capacity
groundspeed
airspeed
low level wind profiles
landing approach methods

18. Distribution Statement
Unclassified - Unlimited

Subject Category 03

19. Security Classif. (of this report)	20. Security Classif. (of this page)	21. No. of Pages	22. Price*
Unclassified	Unclassified	45	$4.50

* For sale by the National Technical Information Service, Springfield, Virginia 22161